

**Characterization of the Human Skeletal Muscle Proteome
by One-dimensional Gel Electrophoresis and HPLC-ESI-MS/MS**

Kurt Højlund^{1,2,§}, Zhengping Yi^{1,3,§*}, Hyonson Hwang^{1,4}, Benjamin Bowen^{1,5}, Natalie Lefort^{1,4},
Charles R. Flynn¹, Paul Langlais^{1,4}, Susan T. Weintraub⁶; and Lawrence J. Mandarino^{1,3,4}

[§]These authors contributed equally to the work.

¹Center for Metabolic Biology, Arizona State University, Tempe, Arizona; ²Diabetes Research Centre, Department of Endocrinology, Odense University Hospital, Odense, Denmark; ³School of Life Sciences, Arizona State University, Tempe, Arizona; ⁴Department of Kinesiology, Arizona State University, Tempe, Arizona; ⁵Harrington Department of Bioengineering, Arizona State University, Tempe, Arizona; ⁶Department of Biochemistry, The University of Texas Health Science Center at San Antonio, San Antonio, Texas

Running title: Human Skeletal Muscle Proteome

Address for Correspondence:

Zhengping Yi, Ph.D.
Center for Metabolic Biology
College of Liberal Arts and Sciences
PO Box 873704
Tempe, Arizona 85287-3704
U.S.A.
Phone: 480-727-7602
FAX: 480-727-6813
Email: zhengping.yi@asu.edu

Summary

Changes in protein abundance in skeletal muscle are central to a large number of metabolic and other disorders, including, and perhaps most commonly, insulin resistance. Proteomic analysis of human muscle is an important approach for gaining insight into the biochemical basis for normal and pathophysiological conditions. However, to date, the number of proteins identified by this approach has been limited, with 107 different proteins being the maximum reported so far. Using a combination of one-dimensional-gel electrophoresis and HPLC-ESI-MS/MS, we identified 954 different proteins in human *vastus lateralis* muscle obtained from 3 healthy, non-obese subjects. In addition to a large number of isoforms of contractile proteins, we detected all proteins involved in the major pathways of glucose and lipid metabolism in skeletal muscle. Mitochondrial proteins accounted for 22% of all proteins identified, including 55 subunits of the respiratory complexes I-V. Moreover, a number of enzymes involved in endocrine and metabolic signaling pathways as well as calcium homeostasis were identified. These results provide the most comprehensive characterization of the human skeletal muscle proteome to date. These data hold promise for future global assessment of quantitative changes in the muscle proteome of patients affected by disorders involving skeletal muscle.

Key words: human skeletal muscle, proteomic analysis, HPLC-ESI-MS/MS, one-dimensional (1D)-gel electrophoresis, tissue profiling, mitochondrion

Abbreviations: Formic acid, FA; acetonitrile, ACN; collision-induced dissociation, CID; oxidative phosphorylation, OXPHOS; Gene Ontology annotation, GO; molecular weight, MW; tandem mass spectrometry, MS/MS.

INTRODUCTION

The percutaneous muscle biopsy technique is an important tool in the diagnosis and management of human muscle disorders and has been used widely to investigate many aspects of cell structure and metabolism in normal and abnormal human muscle (1, 2). There is a lack of comprehensive knowledge of the molecular basis of changes in protein expression that are part of normal physiologic adaptations, such as those that occur during exercise training or age-related sarcopenia, or pathophysiological changes associated with disease processes, including atrophy (caused by disuse, spinal cord injury, or weightlessness), ischemic damage, muscular dystrophies, and insulin resistance. Insulin resistance in skeletal muscle is a condition that is common to obesity, type 2 diabetes, and cardiovascular disease. These diseases affect 25 – 50 million individuals in the United States alone, and many more world-wide. During the past decades, percutaneous needle biopsy of the *vastus lateralis* muscle has played an important role in defining the molecular abnormalities underlying insulin resistance (3-5). On the basis of such studies, an increasing number of genes and proteins in several signaling and metabolic pathways have been implicated in skeletal muscle insulin resistance (3-7). However, the majority of studies have focused on only a limited number of genes and proteins. Other investigators have used the needle muscle biopsy technique to study biochemical, histological, and molecular abnormalities in other common diseases, such as the muscular dystrophies (8).

There is a clear need for approaches capable of evaluating global changes in protein expression and modification. High through-put gene expression technologies such as cDNA microarrays are powerful tools for the study of physiological and pathological conditions with complex or multifactorial underlying mechanisms, proving useful in studies of age-related sarcopenia (9), muscle insulin resistance (10-13), muscular dystrophy (8), denervation (14), and

endurance training (15). However, expression of muscle mRNA may not accurately reflect the abundance of proteins and can give no information regarding their posttranslational modifications (16, 17), indicating the need to correlate the results from global gene expression experiments and measurements of protein abundance.

Although human *vastus lateralis* muscle has been used in thousands of studies within the past decade, only a few proteomic studies have been conducted, combining protein separation by two-dimensional (2D) gel-electrophoresis and protein identification by mass spectrometry (18-23). Previously, the most comprehensive assessment of the human *vastus lateralis* proteome reported only 107 different proteins (18). The high abundance of cytoskeletal and contractile proteins combined with dynamic range issues associated with the 2D-gel approach may be factors that have hampered studies on this topic.

The use of two orthogonal liquid chromatography steps for peptide separation prior to tandem mass spectrometry (MS/MS) (24) has yielded substantial improvements in detection limits, and, consequently, identification of increased numbers of proteins in mammalian tissues (25, 26). Recently, 2D high-performance liquid chromatography electrospray tandem mass spectrometry (HPLC-ESI-MS/MS) was used to analyze the proteome of human beta cells, resulting in the identification of 3,365 unique proteins (27). An alternative to 2D gels and 2D HPLC uses separation by one-dimensional (1D) SDS-PAGE and subsequent protein identification by HPLC-ESI-MS/MS (28, 29). This approach has been shown to be comparable to 2D HPLC-ESI-MS/MS with respect to the number of proteins identified (30). Moreover, it is simpler from a technological point of view and is suitable for clinical studies of small tissue samples obtained *in vivo* by biopsy.

In the present study, we used 1D gel electrophoresis and HPLC-ESI-MS/MS to characterize the proteome of human skeletal muscle obtained using percutaneous needle biopsies of the *vastus lateralis* muscle in healthy volunteers. We identified 954 proteins, including all enzymes participating in the major pathways of glucose and lipid metabolism, a large number of proteins involved in mitochondrial oxidative phosphorylation and calcium homeostasis, and most isoforms of the proteins that constitute the myofibrillar apparatus. As such, the proteins identified in our analyses provide a representation of the major biological functions of skeletal muscle.

EXPERIMENTAL PROCEDURES

Subjects – The skeletal muscle samples used for the proteomics analyses in this study were obtained from three healthy, non-obese volunteers (numbered I – III; age, 30 – 47 years; body mass index, 24 – 28 kg/m²; percent body fat, 23 – 34%) with normal glucose tolerance and no family history of type 2 diabetes. The purpose, nature and potential risks of the study were explained to the participants, and written consent was obtained before participation. The protocol was approved by the Institutional Review Board of Arizona State University.

Muscle preparation, electrophoresis and staining – A percutaneous needle biopsy of the *vastus lateralis* muscle was obtained under local anesthesia, and the muscle biopsy specimen was immediately blotted free of blood, frozen, and stored in liquid nitrogen until use. For protein analysis, the muscle biopsy specimens were homogenized while still frozen in an ice-cold buffer (10 µl/mg tissue) consisting of (final concentrations): 50 mM HEPES, pH 7.6; 150 mM NaCl; 20 mM sodium pyrophosphate; 20 mM β-glycerophosphate; 10 mM NaF; 2 mM sodium

orthovanadate; 2 mM EDTA; 1% Triton; 10% glycerol; 2 mM phenylmethylsulfonyl fluoride; 1 mM MgCl₂; 1 mM CaCl₂; 10 µg/ml leupeptin; and 10 µg/ml aprotinin. A Polytron homogenizer (Brinkman Instruments, Westbury, NY) set on maximum speed for 30 sec was used for homogenization. The homogenate was cooled on ice for 20 min and then centrifuged at 10,000 × g for 20 min at 4 °C; the resulting supernatant was frozen until use. Protein concentrations were determined by the method of Lowry (31). Two experiments were performed. Expt. 1: subject I, 75 µg of muscle lysate, proteins separated on a 10% SDS polyacrylamide gel, and HPLC-MS/MS run in duplicate (Expts. 1-1 and 1-2). Expts. 2-1 and 2-2: 60 µg of muscle lysate proteins from subjects II and III, respectively, were separated on 4 – 20% gradient SDS polyacrylamide gels; proteins were visualized with Coomassie blue (Sigma Chemical Co., St. Louis, MO).

In-gel digestion – The gel lane resulting from each experiment was cut into 20 – 24 slices of approximately equal size. Each slice was cut into 1 mm cubes prior to digestion. The gel pieces were placed in a 0.6-ml polypropylene tube, washed with 400 µl of water, destained twice with 300 µl of 50% acetonitrile (ACN) in 40 mM NH₄HCO₃ and dehydrated with 100% ACN for 15 min. After removal of the ACN by aspiration, the gel pieces were dried in a vacuum centrifuge at 62 °C for 30 min. Trypsin (250 ng; Sigma Chemical Co., St. Louis, MO) in 30 µl of 40 mM NH₄HCO₃ was added and the samples were maintained at 4 °C for 15 min prior to the addition of 50 µl of 40 mM NH₄HCO₃. The digestion was allowed to proceed at 37 °C overnight and was terminated by the addition of 10 µl 5% formic acid (FA). After incubation at 37 °C for an additional 30 min and centrifugation for 1 min, each supernatant was transferred to a clean polypropylene tube. The extraction procedure was repeated using 80 µl of 0.5% FA, and the two extracts were combined. The sample volume was reduced to approximately 5 µl by vacuum centrifugation, and 20 µl of 0.05% heptafluorobutyric acid (HFBA)/1% FA:2%ACN was added.

Mass spectrometry – HPLC-ESI-MS/MS was performed on a hybrid linear ion trap (LTQ)-Fourier Transform Ion Cyclotron Resonance (FTICR) mass spectrometer (LTQ FT; Thermo Fisher; San Jose, CA) fitted with a PicoView™ nanospray source (New Objective, Woburn, MA). The mass spectrometer was calibrated weekly according to manufacturer's instructions, achieving mass accuracy of the calibrants within 2 ppm. On-line capillary HPLC was performed using a Michrom BioResources Paradigm MS4 micro HPLC (Auburn, CA) with a PicoFrit™ column (New Objective; 75 μ m i.d., packed with ProteoPep™ II C18 material, 300 Å). Samples were desalted using an on-line Nanotrap (Michrom BioResources) before being loaded onto the PicoFrit™ column. HPLC separations were accomplished with a linear gradient of 2 to 27% ACN in 0.1 % FA in 70 min, a hold of 5 min at 27% ACN, followed by a step to 50% ACN, hold 5 min and then a step to 80%, hold 5 min; flow rate, 300 nl/min. A “top-10” data-dependent tandem mass spectrometry approach was utilized to identify peptides in which a full scan spectrum (survey scan) was acquired followed by collision-induced dissociation (CID) mass spectra of the 10 most abundant ions in the survey scan. The survey scan was acquired using the FTICR mass analyzer in order to obtain high resolution, high mass accuracy data.

Data analysis and bioinformatics – Tandem mass spectra were extracted from Xcalibur "RAW" files and charge states were assigned using the Extract_MSN script that is a component of Xcalibur 2.0 SR2 (Thermo Fisher; San Jose, CA). Charge states and monoisotopic peak assignments were then verified using DTA-SuperCharge, part of the MSQuant suite of software (msquant.sourceforge.net) (32), before all "DTA" files from each gel lane in an experiment were combined into a single Mascot Generic format file. The fragment mass spectra were then searched against the IPI_HUMAN_v3.27 database (67,528 entries, <http://www.ebi.ac.uk/IPI/>) using Mascot (Matrix Science, London, UK; version 2.2). The false discovery rate was

determined by selecting the option to use a "decoy" randomized search strategy that is available in Mascot v2.2. The search parameters that were used were: 10 ppm mass tolerance for precursor ion masses and 0.5 Da for product ion masses; digestion with trypsin; a maximum of two missed tryptic cleavages; variable modifications of oxidation of methionine and phosphorylation of serine, threonine and tyrosine. Probability assessment of peptide assignments and protein identifications were made through use of Scaffold (version Scaffold-01_06_17, Proteome Software Inc., Portland, OR). Only peptides with $\geq 95\%$ probability were considered. Criteria for protein identification included detection of at least 2 unique identified peptides and a probability score of $\geq 95\%$. Proteins that contained identical peptides and could not be differentiated based on MS/MS analysis alone were grouped. Multiple isoforms of a protein were reported only if they were differentiated by at least one unique peptide with $\geq 95\%$ probability, based on Scaffold analysis. IPI accession numbers for identified proteins were input into the UniProt database (www.pir.uniprot.org) to obtain Gene Ontology annotation (GO).

RESULTS

Characteristics of human skeletal muscle proteome – To obtain a comprehensive proteomic characterization of the human *vastus lateralis* muscle, we carried out HPLC-ESI-MS/MS-based analysis of lysates of whole muscle from which proteins were first fractionated by 1D gel electrophoresis. We first performed duplicate HPLC-ESI-MS/MS analyses (Expts. 1-1 and 1-2) on proteins isolated from the muscle of subject I to assess the reproducibility of the approach. In these analyses, 591 and 577 proteins were identified, respectively, corresponding to a total of 668 unique proteins. There were at least two unique peptides ($\geq 95\%$ confidence) assigned to

each identified protein, all with a confidence level $\geq 95\%$ based on the Scaffold analysis. The false discovery rates as assessed by Mascot searching of a randomized database were 3.1% and 3.4%, respectively. Among these proteins, 500 were identified in both Expts. 1-1 and 1-2, giving a reproducibility rate of approximately 75%. Data analysis showed that the three major isoforms of myosin heavy-chain (myosin 1, 2 and 7) comprised approximately 42% of the total spectra, indicating that the analytical space taken up by these myosin isoforms may hamper identification of other proteins that migrate similarly in SDS-polyacrylamide gels. In an attempt to minimize this, in subsequent analyses for subjects II and III, we used gradient gels (4 – 20%) to obtain a better separation of proteins; after separation on the gradient gels, we identified 571 and 616 proteins for subjects II and III, respectively; the proportion of spectra assigned to the 3 major myosin heavy-chain isoforms was reduced to $\sim 32\%$. The false discovery rate was 5.6 % and 5.2%, respectively. A total of 741 unique proteins were identified in the samples isolated from subjects II and III, with 446 of them (60%) identified in the samples from both subjects. Combining the results from all experiments for the three subjects resulted in a total of 954 proteins after redundancy reduction. To our knowledge, the proteins reported here constitute the largest catalog of the healthy human skeletal muscle proteome to date. A detailed list of all proteins identified in this study together with their IPI ID, molecular weight, sequence coverage, and number of unique peptides assigned to each protein are provided as Supplemental information (Supplemental Table 1). For each identified peptide sequence, we have included the following in Supplemental Table 2: modifications, flank residues, precursor mass, charge and mass error observed, the best Mascot score and best peptide identification probability.

Among the proteins identified in this study, numerous entries derived from the protein identification searches had multiple IPI IDs. In many cases, assignment of multiple IDs results

from the potential presence of protein isoforms which cannot be distinguished on the basis of unique peptides. In our results tables, protein with multiple IDs were assigned to a “protein group” (see Supplemental Table 1). Proteins that were attributed a unique IPI ID are listed as a single-entry protein group. As can be seen from Supplemental Table 1, by performing the analysis in this manner, there were 954 protein groups. Among them, the majority (562) had one IPI ID, 230 had two associated IPI IDs and 162 had more than two associated IPI IDs. For 354 out of 392 protein groups containing two or more IPI IDs, the corresponding proteins are known to be translated from the same gene. For protein groups with multiple IPI IDs, the minimum, maximum and mean of molecular weights (MW) and the number of amino acids in each protein sequence are listed in Supplemental Table1.

The MW distribution of all 954 identified proteins is shown in Figure 1A. Nearly one-third of the identified proteins have a MW within the range of 20 – 40 kDa, and more than two-thirds are below 60 kDa. Proteins ranged from 6.1 kDa (cardiac phospholamban) to 3,823 kDa (titin). We found 11 proteins with a MW less than 10 kDa and 114 greater than 100 kDa. Thus, 13% of the identified proteins were outside of the typical separation limits of 2D gel electrophoresis, which has optimum resolution in the 10 to 100 kDa range.

The subcellular location of 776 proteins could be assigned based on the GO information obtained from the UniProt database, while 178 remained unassigned (Figure 1B). Fifty-nine percent of the identified proteins could be assigned to cytoplasm, representing the predominant subcellular location of all identified proteins in this study. It has been estimated that mitochondrial proteins comprise 4.8% of the total human proteome (33). However, in skeletal muscle, we found that 212 of the 954 proteins detected (22%) could be attributed to the

mitochondrion. Nuclear proteins represented the third largest group, with 17% of all identified proteins.

Pathway analysis – From the large number of proteins identified in our analyses, we decided to evaluate the potential applicability of this HPLC-ESI-MS/MS-based proteomic approach for quantitative assessment of skeletal muscle proteins in future studies aimed at elucidating the mechanism underlying changes in muscle structure and metabolism under different physiological and pathophysiological conditions. To do this we examined the representation of the major metabolic pathways (glucose and lipid metabolism, electron transport and oxidative phosphorylation), calcium homeostasis, myofibrillar apparatus and components of IGF and insulin signaling among the proteins we identified.

Glucose and lipid metabolism – All enzymes involved in the glycolytic pathway, glycogen metabolism and the citric acid cycle were identified in these experiments (Figures 2A – C). Moreover, we identified several subunits of four kinases and one major phosphatase (PP1, serine/threonine-protein phosphatase) known to be involved in regulation of the phosphorylation of enzymes such as glycogen synthase or glycogen phosphorylase. In addition, the majority of proteins that are crucial for the activation and transport of fatty acids into the mitochondrion and subsequent degradation in the β -oxidation pathway were identified (Figure 2D). These include enzymes involved in the oxidation of long-chain, medium-chain and short-chain activated fatty acids as well as enzymes required for the oxidation of unsaturated fatty acids.

Electron transport and phosphorylation – The major role of electron transport complexes I – IV is transfer of electrons coupled with proton pumping, with the ultimate goal of enabling oxidative phosphorylation (OXPHOS)—the final step in energy production. Many of the subunits that make up complexes I – V are embedded in the inner membrane of mitochondria

and are, therefore, often more difficult to extract from their membrane environment. In our experiments, we identified 55 (Table 1) of the 88 known subunits of these complexes (34, 35). Many of the subunits in complexes I – V are of low-molecular weight, which may explain why a smaller number of these subunits was identified in our experiments using 10% gels [29 in Expt. 1-1, and 20 in Expt. 1-2 (subject I)] compared to the experiments using the gradient (4 – 20%) gels [41 in Expt. 2-1 (subject II) and 51 in Expt. 2-2 (subject III)]. Several mitochondrial carrier and transfer proteins were also identified in our analyses.

The phosphocreatine/creatine (PCr/Cr) pool is the major source of high energy phosphate bonds for ATP replenishment in skeletal muscle in response to energy-dependent activities such as muscle contraction. Regulation of this reservoir involves a number of enzymes, all of which were identified in this study (36). These enzymes included the catalytic α -2 and the regulatory γ -1 subunits of AMPK kinase, two cytosolic isoforms of creatine kinase (M and B), the mitochondrial creatine kinase isoform, two adenylate kinase isoforms, ADP/ATP translocase and three isoforms of porin (Supplemental Table 1). Together these enzymes have been suggested to comprise a PCr/Cr shuttle, which ensures an efficient mechanism by which PCr can be resynthesized by mitochondrial ATP synthesis (36).

Calcium homeostasis – Calcium homeostasis and calcium-dependent signaling in skeletal muscle play major roles in a number of cellular processes such as contraction, apoptosis, the adiponectin-AMPK signaling pathway, insulin-mediated glucose uptake, and mitochondrial biogenesis and function (37-41) In the present study, we identified three members of the voltage-dependent calcium channel complex, the ryanodine receptor 1, calmodulin and several important calcium/calmodulin binding or regulated proteins (Table 2). These proteins include two subunits of the phosphatase, calcineurin A, all four subunits of calcium/calmodulin dependent kinase II

(CaMKII), cardiac phospholamban, and the two major calcium ATPases (SERCA1 and 2). We also identified a calcium-regulated receptor, T-cadherin, which has been suggested to be a potential adiponectin receptor (42), and the calcium binding protein, MO25, which is a member of the LKB1-STRADA-MO25 complex regulating phosphorylation of AMPK.

Insulin and IGF-I signaling – Insulin and IGF-I have significant metabolic and growth promoting roles in skeletal muscle, and their respective signaling pathways are involved in skeletal muscle insulin resistance. Among the proteins currently believed to mediate the effect of insulin and IGF-I on glucose transport, glycogen synthesis, and protein synthesis in skeletal muscle (3-7, 43), we identified the glycogen-targeting subunit of PP1 (PP1g), several Rab proteins involved in GLUT4 translocation, and a number of eukaryotic translation initiation and elongation factors and ribosomal protein S6 kinase involved in protein synthesis (Supplemental Table 1). Moreover, a number of kinases, phosphatases and other proteins known to modulate insulin and IGF-I signaling (3) were found. In addition to those already mentioned, three subunits of another phosphatase, PP2A, MAP kinase, MAP kinase kinases and serine/threonine kinases were identified. A number of cytosolic and mitochondrial chaperones were also found. Of these, HSP90 and its co-chaperone cdc37, in particular, have been suggested to interact with PDK1 and Akt (44); both are elements of insulin and IGF-I signaling. Moreover, four isoforms of the phosphoserine/phosphothreonine binding 14-3-3 proteins were identified. They have been reported to bind to insulin receptor substrate (IRS)-1, IRS-2, and PDK1 and to modulate the activities of IRS-1 associated PI3-kinase and PDK1 (3).

Extracellular matrix (ECM) and contractile proteins – Muscle adaptation in response to a number of physiological and pathophysiological conditions involves changes in ECM and contractile proteins (13, 14, 45). Among ECM proteins, we found three α -subunits of type VI

collagen, fibronectin, decorin, lumican and prolargin. Multiple isoforms of proteins constituting the myofibrillar apparatus were identified, including four actin isoforms, three α -actinin isoforms, nine myosin heavy chain isoforms, eight myosin light chains isoforms, two myomesin isoforms and titin. Moreover, both slow and fast skeletal muscle isoforms of troponin I, C and T in the troponin complex were identified together with several tropomyosin and tropomodulin isoforms.

Phosphorylation sites – Although no attempt was made to enrich phosphopeptides, 35 phosphorylation sites in 24 proteins were detected with confidence (95 % using Scaffold analysis (Table 3). According to available databases (www.phosphosite.org, www.phospho.elm.eu.org, www.mitocheck.org, www.phosida.com and www.expasy.ch) and existing literature, 16 of these phosphorylation sites have been reported before, whereas 19 phosphorylation sites in 13 proteins appear to be novel. These new phosphorylation sites were identified on proteins critical for muscle metabolism such as aldolase A, alpha/beta-enolase, glyceraldehyde-3-phosphate dehydrogenase, creatine kinase M, and glycogen phosphorylase as well as on muscle-specific proteins such as myoglobin, myomesin 1, myosin binding protein C and LIM domain-binding protein 3.

DISCUSSION

A number of previous proteomic studies of human skeletal muscle have been accomplished using protein separation by 2D-gel electrophoresis with subsequent identification using MALDI-TOF/MS and/or HPLC-ESI-MS/MS analyses (18-23). Most are comparative studies reporting only proteins that are differentially regulated in conditions such as type 2 diabetes (23), obesity

(22), Tibetans at high altitude (20), and aging (21), or in comparisons between different muscle fiber types (19). The proteins reported in those studies represent mainly highly-abundant structural or metabolic proteins. Of the 62 different proteins reported in these five studies (19-23), 59 were also identified in the present investigation. In comparative experiments that employ 2-D gel electrophoresis, differences in spot staining intensity are used as a measure of changes in protein expression. However, since a large number of proteins are present in more than one differently migrating protein spot (due to the presence of different isoforms or post-translational modifications), it is difficult to get a reliable estimate of the total content of a specific protein by the 2D gel approach (19, 23). Furthermore, those studies focus primarily on differentially regulated proteins, and, thus, many other proteins that are not altered in abundance or are present at too low a level to be easily quantified by spot analysis often are not identified.

In the past, there are only a limited number of reports in the literature on characterization of the human skeletal muscle proteome (18, 46). To date, the most comprehensive list of proteins of human *vastus lateralis* muscle has been reported by Gelfi and co-workers (18) who used 2D-gel electrophoresis, MALDI-TOF/MS and HPLC-ESI-MS/MS. Approximately 500 protein spots were visualized by silver-staining, and 150 spots were excised, resulting in identification of 107 different proteins. Of those 107 proteins, 101 were identified in the present study. In a more recent report using two-dimensional difference gel electrophoresis (DIGE) to characterize the effects of aging on the human skeletal muscle, approximately 2,700 protein spots were visualized, 52 of which were differentially expressed, and 39 proteins were identified (21). However, in addition to difficulties in identifying proteins at the extremes of the MW and pI ranges, a major weakness in the 2D-gel approach is in detection and subsequent identification of low-abundance proteins. Moreover, identification of proteins in all spots detected in a 2D gel

[such as the 2,700 reported by Gelfi et al (21)] would be extremely labor-intensive, even with robotic processing.

Nuclear extracts from human muscle specimens of unspecified origin obtained from surgery or autopsies have been analyzed by 2D-HPLC-ESI-MS/MS, resulting in the identification of 192 different muscle proteins (46). In our analysis of whole cell lysates of human *vastus lateralis* muscle, we identified 116 of these nuclear proteins. Among those we did not identify, half were either hypothetical proteins or were assigned to the mouse database.

For our analysis of the human muscle protein, we elected to apply a relatively simple approach based on 1D gel electrophoresis and HPLC-ESI-MS/MS analysis—a strategy that has been successful in studies of human cell lines (28, 29) and can be used with very small amounts of tissue in clinical studies. Using this approach, we identified 954 different proteins, which to our knowledge, represents the most comprehensive identification of proteins in human *vastus lateralis* muscle. This list includes a large number of membrane-associated and low molecular weight proteins, indicating less issues in this regard compared to 2D gel electrophoresis. In Figure 1B is a comparison of the MW range of proteins identified in our study with those listed in the IPI human database. If the MW distribution of proteins in human muscle is the same as the in the human proteome cataloged in the IPI human database, we identified a lower than expected proportion of proteins under 20 kDa. This suggests that either there is a lack of detection of these proteins by our approach or else the molecular weights of proteins in human muscle do not parallel those of the entire proteome.

Mechanisms underlying changes in muscle structure and metabolism during different physiological and pathophysiological conditions have traditionally been studied by focusing on small numbers of genes or proteins. Transcriptional profiling has been applied to define the

molecular signature of denervation, immobilization, exercise-training, age-related sarcopenia, insulin resistance and muscular dystrophy (8-15, 45). However, global profiling of temporal changes in metabolic enzymes and structural proteins and their posttranslational modifications in skeletal muscle *in vivo* has been limited by the lack of appropriate proteomic technology. The present study shows that it is feasible to obtain a comprehensive identification of human skeletal muscle proteins with full representation of enzymes involved in glucose and lipid metabolism, a high number of mitochondrial proteins, including 55 OXPHOS subunits and carrier/transport proteins involved in ATP synthesis, and multiple proteins involved in calcium homeostasis including calmodulin, CaMKII, phospholamban and calcineurin A, which have been shown to play a role in insulin-mediated glucose transport, mitochondrial biogenesis and transcriptional regulation of lipid oxidation genes (37-41). As expected, a diversity of isoforms of myofibrillar and cytoskeletal proteins was found, reflecting the mixed fiber type composition of the human *vastus lateralis* muscle. Of potential importance to future studies regarding insulin resistance, we were able to identify several kinases, phosphatases and enzymes known to regulate glycogen synthase, glucose transport, and protein synthesis and to modulate proximal insulin and IGF-I signaling (3-7, 43). Moreover, 16 known and 19 previously unreported phosphorylation sites were detected without phosphopeptide enrichment.

An analysis of the activity and subunit composition of mitochondria plays a central role in the diagnosis of mitochondrial myopathies, the pathophysiology of type 2 diabetes and age-related sarcopenia, and physiological responses to exercise. In addition to the citric acid cycle, β -oxidation and OXPHOS, mitochondrial proteins are involved in a variety of cellular processes including intracellular calcium homeostasis, programmed cell death (apoptosis) and ion homeostasis. The 212 mitochondrial proteins identified in the present study represent, to our

knowledge, the most comprehensive proteomic identification of mitochondrial proteins of human skeletal muscle reported to date. In a proteomic study of rat mitochondria purified from skeletal muscle, heart, and liver, 689 proteins were identified, with only small differences found between skeletal muscle and heart (47). The most extensive evaluation of human mitochondrial proteins identified 680 proteins in purified heart mitochondria (48), utilizing 40 mg of purified mitochondria as starting material and 701 HPLC-ESI-MS/MS analyses. Based on those results, it is likely that we would improve our coverage of the estimated 1,500 human mitochondrial proteins (33) if muscle mitochondria were isolated prior to 1D-gel electrophoresis and HPLC-ESI-MS/MS. The finding that mitochondrial proteins accounted for 21% of all skeletal muscle proteins identified in the present study, compared to 4.8% in the total human proteome (33) may reflect the critical role that mitochondria play for energy metabolism in skeletal muscle and the enormous demand for ATP elicited by muscle contraction.

In conclusion, this study represents the first application of 1D-gel electrophoresis and HPLC-ESI-MS/MS for analysis of the human skeletal muscle proteome. Using only 60 – 70 μ g of total protein from 3 lean subjects in less than 90 HPLC-ESI-MS/MS runs, we provide the most comprehensive proteome coverage of human skeletal muscle to date. This includes the largest catalogue of mitochondrial proteins in human skeletal muscle. It is important to emphasize that the quantity of protein from each subject that was used in these experiments represents a small fraction of the muscle obtained by percutaneous needle biopsy. These data demonstrate the utility of this relatively simple proteomic approach for analysis of small human tissue samples, making it a potentially valuable tool in elucidating changes in the proteome associated with human disease.

Acknowledgements – This work was supported by NIH grants R01DK47936 and R01DK66483 (LJM), a Mentor-Based Postdoctoral Fellowship Award from the American Diabetes Association (LJM). KH was funded by grants from the Danish Diabetes Association, and the Danish Medical Research Council. We thank Mr. Michael Sweet, an undergraduate student in our group for initial data analysis.

References

1. Bergstrom, J. (1975) Percutaneous needle biopsy of skeletal muscle in physiological and clinical research. *Scand. J. Clin. Lab. Invest.* 35, 609-616.
2. Edwards, R., Young, A. and Wiles, M. (1980) Needle biopsy of skeletal muscle in the diagnosis of myopathy and the clinical study of muscle function and repair. *N. Engl. J. Med.* 302, 261-271.
3. Hojlund, K. and Beck-Nielsen, H. (2006) Impaired glycogen synthase activity and mitochondrial dysfunction in skeletal muscle. Markers or mediators in type 2 diabetes. *Current Diabetes Reviews.* 2, 375-395.
4. Krebs, M. and Roden, M. (2005) Molecular mechanisms of lipid-induced insulin resistance in muscle, liver and vasculature. *Diabetes Obes. Metab.* 7, 621-632.
5. Lowell, B. B. and Shulman, G. I. (2005) Mitochondrial dysfunction and type 2 diabetes. *Science.* 307, 384-387.
6. Pirola, L., Johnston, A. M. and Van Obberghen, E. (2004) Modulation of insulin action. *Diabetologia.* 47, 170-184.
7. Kelley, D. E. and Mandarino, L. J. (2000) Fuel selection in human skeletal muscle in insulin resistance: a reexamination. *Diabetes.* 49, 677-683.
8. Winokur, S. T., Chen, Y. W., Masny, P. S., Martin, J. H., Ehmsen, J. T., Tapscott, S. J., van der Maarel, S. M., Hayashi, Y. and Flanigan, K. M. (2003) Expression profiling of FSHD muscle supports a defect in specific stages of myogenic differentiation. *Hum. Mol. Genet.* 12, 2895-2907.
9. Giresi, P. G., Stevenson, E. J., Theilhaber, J., Koncarevic, A., Parkington, J., Fielding, R. A. and Kandarian, S. C. (2005) Identification of a molecular signature of sarcopenia. *Physiol. Genomics.* 21, 253-263.
10. Patti, M. E., Butte, A. J., Crunkhorn, S., Cusi, K., Berria, R., Kashyap, S., Miyazaki, Y., Kohane, I., Costello, M., Saccone, R., Landaker, E. J., Goldfine, A. B., Mun, E., DeFronzo, R., Finlayson, J., Kahn, C. R. and Mandarino, L. J. (2003) Coordinated reduction of genes of oxidative metabolism in humans with insulin resistance and diabetes: Potential role of PGC1 and NRF1. *Proc. Natl. Acad. Sci. U S A.* 100, 8466-8471.
11. Mootha, V. K., Lindgren, C. M., Eriksson, K. F., Subramanian, A., Sihag, S., Lehar, J., Puigserver, P., Carlsson, E., Ridderstrale, M., Laurila, E., Houstis, N., Daly, M. J., Patterson, N., Mesirov, J. P., Golub, T. R., Tamayo, P., Spiegelman, B., Lander, E. S., Hirschhorn, J. N., Altshuler, D. and Groop, L. C. (2003) PGC-1alpha-responsive genes involved in oxidative phosphorylation are coordinately downregulated in human diabetes. *Nat. Genet.* 34, 267-273.

12. Sreekumar, R., Halvatsiotis, P., Schimke, J. C. and Nair, K. S. (2002) Gene expression profile in skeletal muscle of type 2 diabetes and the effect of insulin treatment. *Diabetes*. 51, 1913-1920.
13. Richardson, D. K., Kashyap, S., Bajaj, M., Cusi, K., Mandarino, S. J., Finlayson, J., DeFronzo, R. A., Jenkinson, C. P. and Mandarino, L. J. (2005) Lipid infusion decreases the expression of nuclear encoded mitochondrial genes and increases the expression of extracellular matrix genes in human skeletal muscle. *J. Biol. Chem.* 280, 10290-10297.
14. Batt, J., Bain, J., Goncalves, J., Michalski, B., Plant, P., Fahnestock, M. and Woodgett, J. (2006) Differential gene expression profiling of short and long term denervated muscle. *Faseb J.* 20, 115-117.
15. Teran-Garcia, M., Rankinen, T., Koza, R. A., Rao, D. C. and Bouchard, C. (2005) Endurance training-induced changes in insulin sensitivity and gene expression. *Am. J. Physiol. Endocrinol. Metab.* 288, E1168-1178.
16. Anderson, L. and Seilhamer, J. (1997) A comparison of selected mRNA and protein abundances in human liver. *Electrophoresis*. 18, 533-537.
17. Gygi, S. P., Rochon, Y., Franza, B. R. and Aebersold, R. (1999) Correlation between protein and mRNA abundance in yeast. *Mol. Cell. Biol.* 19, 1720-1730.
18. Gelfi, C., De Palma, S., Cerretelli, P., Begum, S. and Wait, R. (2003) Two-dimensional protein map of human vastus lateralis muscle. *Electrophoresis*. 24, 286-295.
19. Capitanio, D., Vigano, A., Ricci, E., Cerretelli, P., Wait, R. and Gelfi, C. (2005) Comparison of protein expression in human deltoideus and vastus lateralis muscles using two-dimensional gel electrophoresis. *Proteomics*. 5, 2577-2586.
20. Gelfi, C., De Palma, S., Ripamonti, M., Eberini, I., Wait, R., Bajracharya, A., Marconi, C., Schneider, A., Hoppeler, H. and Cerretelli, P. (2004) New aspects of altitude adaptation in Tibetans: a proteomic approach. *Faseb J.* 18, 612-614.
21. Gelfi, C., Vigano, A., Ripamonti, M., Pontoglio, A., Begum, S., Pellegrino, M. A., Grassi, B., Bottinelli, R., Wait, R. and Cerretelli, P. (2006) The human muscle proteome in aging. *J. Proteome Res.* 5, 1344-1353.
22. Hittel, D. S., Hathout, Y., Hoffman, E. P. and Houmard, J. A. (2005) Proteome analysis of skeletal muscle from obese and morbidly obese women. *Diabetes*. 54, 1283-1288.
23. Hojlund, K., Wrzesinski, K., Larsen, P. M., Fey, S. J., Roepstorff, P., Handberg, A., Dela, F., Vinten, J., McCormack, J. G., Reynet, C. and Beck-Nielsen, H. (2003) Proteome analysis reveals phosphorylation of ATP synthase beta -subunit in human skeletal muscle and proteins with potential roles in type 2 diabetes. *J. Biol. Chem.* 278, 10436-10442.
24. Washburn, M. P., Wolters, D. and Yates, J. R., 3rd (2001) Large-scale analysis of the yeast proteome by multidimensional protein identification technology. *Nat. Biotechnol.* 19, 242-247.

25. Jacobs, J. M., Mottaz, H. M., Yu, L. R., Anderson, D. J., Moore, R. J., Chen, W. N., Auberry, K. J., Strittmatter, E. F., Monroe, M. E., Thrall, B. D., Camp, D. G., 2nd and Smith, R. D. (2004) Multidimensional proteome analysis of human mammary epithelial cells. *J. Proteome Res.* 3, 68-75.
26. Pan, Y., Kislinger, T., Gramolini, A. O., Zvaritch, E., Kranias, E. G., MacLennan, D. H. and Emili, A. (2004) Identification of biochemical adaptations in hyper- or hypocontractile hearts from phospholamban mutant mice by expression proteomics. *Proc. Natl. Acad. Sci. U S A.* 101, 2241-2246.
27. Metz, T. O., Jacobs, J. M., Gritsenko, M. A., Fontes, G., Qian, W. J., Camp, D. G., 2nd, Poitout, V. and Smith, R. D. (2006) Characterization of the human pancreatic islet proteome by two-dimensional LC/MS/MS. *J. Proteome Res.* 5, 3345-3354.
28. Schirle, M., Heurtier, M. A. and Kuster, B. (2003) Profiling core proteomes of human cell lines by one-dimensional PAGE and liquid chromatography-tandem mass spectrometry. *Mol. Cell. Proteomics.* 2, 1297-1305.
29. Rezaul, K., Wu, L., Mayya, V., Hwang, S. I. and Han, D. (2005) A systematic characterization of mitochondrial proteome from human T leukemia cells. *Mol. Cell. Proteomics.* 4, 169-181.
30. Lasonder, E., Ishihama, Y., Andersen, J. S., Vermunt, A. M., Pain, A., Sauerwein, R. W., Eling, W. M., Hall, N., Waters, A. P., Stunnenberg, H. G. and Mann, M. (2002) Analysis of the Plasmodium falciparum proteome by high-accuracy mass spectrometry. *Nature.* 419, 537-542.
31. Lowry, O. H., Rosebrough, N. J., Farr, A. L. and Randall, R. J. (1951) Protein measurement with the Folin phenol reagent. *J. Biol. Chem.* 193, 265-275.
32. Foster, L. J., Rudich, A., Talior, I., Patel, N., Huang, X., Furtado, L. M., Bilan, P. J., Mann, M. and Klip, A. (2006) Insulin-dependent interactions of proteins with GLUT4 revealed through stable isotope labeling by amino acids in cell culture (SILAC). *J. Proteome Res.* 5, 64-75.
33. Guda, C., Fahy, E. and Subramaniam, S. (2004) MITOPRED: a genome-scale method for prediction of nucleus-encoded mitochondrial proteins. *Bioinformatics.* 20, 1785-1794.
34. Carroll, J., Fearnley, I. M., Skehel, J. M., Shannon, R. J., Hirst, J. and Walker, J. E. (2006) Bovine complex I is a complex of 45 different subunits. *J. Biol. Chem.* 281, 32724-32727.
35. Scheffler, I. E. (2004) *The Human OXPHOS system: Structure, Function, Physiology*, Landes Bioscience and Kluwer Academic/Plenum Publishers.
36. Neumann, D., Schlattner, U. and Wallimann, T. (2003) A molecular approach to the concerted action of kinases involved in energy homeostasis. *Biochem. Soc. Trans.* 31, 169-174.
37. Gunter, T. E., Yule, D. I., Gunter, K. K., Eliseev, R. A. and Salter, J. D. (2004) Calcium and mitochondria. *FEBS Lett.* 567, 96-102.

38. Konstantopoulos, N., Marcuccio, S., Kyi, S., Stoichevska, V., Castelli, L. A., Ward, C. W. and Macaulay, S. L. (2007) A purine analog kinase inhibitor, calcium/calmodulin-dependent protein kinase II inhibitor 59, reveals a role for calcium/calmodulin-dependent protein kinase II in insulin-stimulated glucose transport. *Endocrinology*. 148, 374-385.
39. Lanner, J. T., Katz, A., Tavi, P., Sandstrom, M. E., Zhang, S. J., Wretman, C., James, S., Fauconnier, J., Lannergren, J., Bruton, J. D. and Westerblad, H. (2006) The role of Ca²⁺ influx for insulin-mediated glucose uptake in skeletal muscle. *Diabetes*. 55, 2077-2083.
40. Long, Y. C., Glund, S., Garcia-Roves, P. M. and Zierath, J. R. (2007) Calcineurin regulates skeletal muscle metabolism via coordinated changes in gene expression. *J. Biol. Chem.* 282, 1607-1614.
41. Wu, H., Kanatous, S. B., Thurmond, F. A., Gallardo, T., Isotani, E., Bassel-Duby, R. and Williams, R. S. (2002) Regulation of mitochondrial biogenesis in skeletal muscle by CaMK. *Science*. 296, 349-352.
42. Hug, C., Wang, J., Ahmad, N. S., Bogan, J. S., Tsao, T. S. and Lodish, H. F. (2004) T-cadherin is a receptor for hexameric and high-molecular-weight forms of Acrp30/adiponectin. *Proc. Natl. Acad. Sci. U S A*. 101, 10308-10313.
43. Solomon, A. M. and Bouloux, P. M. (2006) Modifying muscle mass - the endocrine perspective. *J. Endocrinol.* 191, 349-360.
44. Basso, A. D., Solit, D. B., Chiosis, G., Giri, B., Tsihchlis, P. and Rosen, N. (2002) Akt forms an intracellular complex with heat shock protein 90 (Hsp90) and Cdc37 and is destabilized by inhibitors of Hsp90 function. *J. Biol. Chem.* 277, 39858-39866.
45. Urso, M. L., Scrimgeour, A. G., Chen, Y. W., Thompson, P. D. and Clarkson, P. M. (2006) Analysis of human skeletal muscle after 48 h immobilization reveals alterations in mRNA and protein for extracellular matrix components. *J. Appl. Physiol.* 101, 1136-1148.
46. Cagney, G., Park, S., Chung, C., Tong, B., O'Dushlaine, C., Shields, D. C. and Emili, A. (2005) Human tissue profiling with multidimensional protein identification technology. *J. Proteome Res.* 4, 1757-1767.
47. Reifschneider, N. H., Goto, S., Nakamoto, H., Takahashi, R., Sugawa, M., Dencher, N. A. and Krause, F. (2006) Defining the mitochondrial proteomes from five rat organs in a physiologically significant context using 2D blue-native/SDS-PAGE. *J. Proteome Res.* 5, 1117-1132.
48. Taylor, S. W., Fahy, E., Zhang, B., Glenn, G. M., Warnock, D. E., Wiley, S., Murphy, A. N., Gaucher, S. P., Capaldi, R. A., Gibson, B. W. and Ghosh, S. S. (2003) Characterization of the human heart mitochondrial proteome. *Nat. Biotechnol.* 21, 281-286.

Legends

Figure 1. Molecular weight distribution and subcellular location of human skeletal muscle proteins. (A): Distribution of the 954 proteins identified in human vastus lateralis muscle (closed bars) compared to all proteins in the IPI human database (open bars) relative to their predicted molecular weight and subcellular location. (B): Distribution of the 954 identified proteins according to Gene Ontology (GO) annotation. In cases where an identified protein group contained more than one IPI ID, the average molecular weight was used.

Figure 2. Proteomic coverage of major enzymes involved in glucose and lipid metabolism in human skeletal muscle. (A), Isoforms and/or subunits of enzymes involved in glycogen metabolism, (B), glycolysis, (C), citric acid cycle, and (D), fatty acid transport into and oxidation in mitochondria. Proteins identified are shown in gray boxes, and the associated gene names, maximum observed number of unique peptides, and sequence coverage are presented in adjacent white boxes.

Table I *Proteins involved in oxidative phosphorylation (OXPHOS) identified in human skeletal muscle.* Proteins were separated by one-dimensional gel electrophoresis and identified by HPLC-ESI-MS/MS in four experiments using skeletal muscle from three non-obese, healthy subjects

Protein	Gene name	MW (kDa) ¹	Max. unique peptides ²	Max. sequence coverage (%) ²
Complex I				
NADH dehydrogenase 1 subunit C2	NDUFC2	14	2	17
NADH dehydrogenase 1 α subcomplex subunit 2	NDUFA2	11	3	20
NADH dehydrogenase 1 α subcomplex subunit 4	NDUFA4	9	2	22
NADH dehydrogenase 1 α subcomplex subunit 5	NDUFA5	14	3	31
NADH dehydrogenase 1 α subcomplex subunit 6	NDUFA6	18	2	12
NADH dehydrogenase 1 α subcomplex subunit 7	NDUFA7	13	3	35
NADH dehydrogenase 1 α subcomplex subunit 8	NDUFA8	20	3	30
NADH dehydrogenase 1 α subcomplex subunit 9	NDUFA9	43	7	26
NADH dehydrogenase 1 α subcomplex subunit 10	NDUFA10	41	6	16
NADH dehydrogenase 1 α subcomplex subunit 12	NDUFA12	17	2	20
NADH dehydrogenase 1 α subcomplex subunit 13	NDUFA13	26	4	22
NADH dehydrogenase 1 β subcomplex subunit 3	NDUFB3	11	2	21
NADH dehydrogenase 1 β subcomplex subunit 4	NDUFB4	15	2	17
NADH dehydrogenase 1 β subcomplex subunit 5	NDUFB5	20	3	12
NADH dehydrogenase 1 β subcomplex subunit 7	NDUFB7	16	2	12
NADH dehydrogenase 1 β subcomplex subunit 8	NDUFB8	20	2	22
NADH dehydrogenase 1 β subcomplex subunit 9	NDUFB9	21	3	27
NADH dehydrogenase 1 β subcomplex subunit 10	NDUFB10	21	4	31
NADH dehydrogenase 1 β subcomplex subunit 11 isoform 2	NDUFB11	18	2	21
NADH-ubiquinone oxidoreductase 9.6 kDa subunit	NDUFAB1	17	3	15
NADH-ubiquinone oxidoreductase 75 kDa subunit	NDUFS1	79	21	36
NADH dehydrogenase iron-sulfur protein 2	NDUFS2	53	15	45
NADH dehydrogenase iron-sulfur protein 3	NDUFS3	30	5	20
NADH dehydrogenase iron-sulfur protein 4	NDUFS4	20	2	15
NADH dehydrogenase iron-sulfur protein 5	NDUFS5	12	3	25
NADH dehydrogenase iron-sulfur protein 7	NDUFS7	28	3	15
NADH dehydrogenase iron-sulfur protein 8	NDUFS8	24	3	15
NADH dehydrogenase flavoprotein 1 isoform 1	NDUFV1	50	12	24
NADH dehydrogenase flavoprotein 2	NDUFV2	26	2	11
NADH dehydrogenase flavoprotein 3	NDUFV3	51	2	7
Complex II				
Succinate dehydrogenase flavoprotein subunit	SDHA	73	12	22
Succinate dehydrogenase iron-sulfur protein	SDHB	32	6	24
Complex III				
Ubiquinol-cytochrome c reductase iron-sulfur subunit	UQCRC1	30	5	22
Cytochrome c1, heme protein	CYC1	35	5	16
Ubiquinol-cytochrome-c reductase complex core protein I	UQCRC1	53	11	28
Ubiquinol-cytochrome-c reductase complex core protein 2	UQCRC2	48	13	41
Ubiquinol-cytochrome c reductase complex 14 kDa protein	UQCRB	13	3	32
Ubiquinol-cytochrome c reductase complex 7.2 kDa protein	UCRC	7	2	38
Complex IV				
Cytochrome c oxidase subunit 2	COX2	26	6	39
Cytochrome c oxidase subunit 4 isoform 1	COX4I1	20	8	46
Cytochrome c oxidase subunit 5A	COX5A	17	3	25
Cytochrome c oxidase subunit 5B	COX5B	14	2	9
Cytochrome c oxidase polypeptide Vic	COX6C	9	5	37
Cytochrome c oxidase polypeptide VIIa-Heart	COX7A1	11	2	29

Protein	Gene name	MW (kDa) ¹	Max. unique peptides ²	Max. sequence coverage (%) ²
Complex V				
ATP synthase B chain	ATP5F1	26	9	36
ATP synthase D chain isoform 1	ATP5H	18	9	52
ATP synthase E chain	ATP5I	8	3	50
ATP synthase F chain isoform 2	ATP5J2	8	2	44
ATP synthase subunit G	ATP5L	11	7	54
ATP synthase subunit α	ATP5A1	60	39	62
ATP synthase subunit β	ATP5B	57	40	75
ATP synthase δ chain	ATP5D	17	3	23
ATP synthase γ chain isoform heart	ATP5C1	33	5	18
ATP synthase coupling factor 6	ATP5J	13	5	45
ATP synthase O subunit (OSCP)	ATP5O	23	6	35
Carrier/transfer proteins				
Cytochrome <i>c</i>	CYCS	12	6	50
Phosphate carrier protein isoform A	SLC25A3	35	4	12
ADP/ATP translocase 1	SLC25A4	33	10	35
Mitochondrial 2-oxoglutarate/malate carrier protein	SLC25A11	34	7	26
Calcium-binding mitochondrial carrier protein Aralar1	SLC25A12	75	28	52
Electron transfer flavoprotein subunit β	ETFA	35	6	27
Electron transfer flavoprotein subunit β	ETFB	33	9	33
Electron transfer flavoprotein-ubiquinone oxidoreductase	ETFDH	68	9	20
NAD(P) transhydrogenase	NNT	114	11	14

¹MW, molecular weight; the mean molecular weight is shown for proteins with more than one IPI ID.

²Maximum values for one analysis

Table II. *Proteins involved in calcium homeostasis identified in human skeletal muscle.* Proteins were separated by one-dimensional gel electrophoresis and identified by HPLC-ESI-MS/MS in four experiments using skeletal muscle from three non-obese, healthy subjects

Protein	Gene name	MW (kDa) ¹	Max. unique peptides ²	Max. sequence coverage (%) ²
Calcium Channels/Receptors				
Dihydropyridine receptor α 2	CACNA2D1	125	10	13
Voltage-dependent L-type calcium channel α -S1	CACNA1S	212	2	2
Voltage-dependent L-type calcium channel β -1	CACNB1	64	9	23
Ryanodine receptor 1	RYR1	565	8	3
Calcium-Adiponectin-AMPK				
Cadherin 13 (T-cadherin)	CDH13	78	4	8
5'-AMP-activated protein kinase catalytic α -2	PRKAA2	62	5	13
5'-AMP-activated protein kinase regulatory γ -1	PRKAG1	38	4	17
Calcium-binding protein 39 (Protein Mo25)	CAB39	40	6	18
Calcium regulated enzymes				
Calmodulin	CALM1	17	4	42
Calmodulin-dependent calcineurin A α	PPP3CA	58	3	8
Calmodulin-dependent calcineurin A β	PPP3CB	58	4	10
Calcium/calmodulin-dependent protein kinase II α	CAMK2A	54	4	13
Calcium/calmodulin-dependent protein kinase II β	CAMK2B	73	7	13
Calcium/calmodulin-dependent protein kinase II δ	CAMK2D	56	5	15
Calcium/calmodulin-dependent protein kinase II γ	CAMK2G	59	5	13
Cardiac phospholamban	PLN	6	3	23
Sarcoplasmic/endoplasmic reticulum calcium ATPase 1	ATP2A1	103	41	36
Sarcoplasmic/endoplasmic reticulum calcium ATPase 2	ATP2A2	110	42	33
GTP-binding protein RAD	RRAD	33	2	10
Calpain-1 catalytic subunit	CAPN1	82	12	22
Calpain-2 catalytic subunit	CAPN2	80	3	5
Calpain-3	CAPN3	94	7	13
Calpain small subunit 1	CAPNS1	31	4	18
Calcium binding proteins				
Calreticulin	CALR	42	2	9
Calnexin	CANX	68	5	11
Sarcolumenin	SRL	97	20	26
Sarcoplasmic reticulum histidine-rich calcium-binding protein	HRC	81	4	12
Calsequestrin-1	CASQ1	45	15	28
Calsequestrin-2	CASQ2	46	10	29
Annexin A1	ANXA1	39	7	28
Annexin A2	ANXA2	40	15	48
Annexin A4	ANXA4	35	2	8
Annexin A5	ANXA5	36	14	42
Annexin A6	ANXA6	76	32	53
Annexin A7	ANXA7	52	4	11
Annexin A11	ANXA11	54	8	22
S100 calcium-binding protein A1	S100A1	11	2	38
S100 calcium-binding protein A6	S100A6	10	2	17
Copine-3	CPNE3	60	3	7
Gelsolin	GSN	83	12	25

¹MW, molecular weight; the mean molecular weight is shown for proteins with more than one IPI ID.

²Maximum values for one analysis

Table III *Phosphorylation sites in human skeletal muscle proteins identified by HPLC-ESI-MS/MS*. Proteins were separated by one-dimensional gel electrophoresis and phosphorylation sites were identified by HPLC-ESI-MS/MS in four experiments using skeletal muscle from three non-obese, healthy subjects. No phosphopeptide enrichment strategies were employed.

Protein	Gene name	Sequence ¹	Mono-phosphorylation site(s) ²
Aldolase A	ALDOA	²⁹ GILAADESTGSIK ⁴²	S36, T37*, S39
Alpha crystallin family protein	CRYAB	²⁹ RASAPLPLGLSAPGR ⁴²	S31
Alpha/beta-enolase	ENO1/3	³³ AAVPSGASTGIYEALRL ⁵⁰	S40*, T41*, Y44
cAMP-dep. protein kinase regulatory α -1 subunit	PRKAR2A	⁷⁵ TDSREDEISPPPPNPVVK ⁹²	S83
Carbonic anhydrase 3	CA3	⁴⁰ HDPSLQPWSVSYDGGSAK ⁵⁷	S48*
Cardiac phospholamban	PLN	¹⁴ RASTIEMPQQR ²⁵	S16
Cardiac phospholamban	PLN	¹⁴ ASTIEMPQQR ²⁵	T17
Creatine kinase M	CKM	¹⁵⁷ LSVEALNSLTGEFK ¹⁷⁰	S164*
Creatine kinase M	CKM	³²¹ GTGGVDTAAVGSVFDVSNADR ³⁴¹	T322*, T327*, S332*
Gamma filamin variant	FLNC	²²¹¹ LGSFGSITR ²²¹⁹	S2213
Glyceraldehyde-3-phosphate dehydrogenase	GAPDH	¹⁶³ VIHDNFGIVEGLMTTVHAIATQK ¹⁸⁶	T182, T184*
Glycogen phosphorylase, muscle form	PYGM	⁴⁶⁷ TIFKDFYELEPHK ⁴⁷⁹	Y473*
Glycogen synthase, muscle	GYS1	⁷⁰⁸ RNSVDATSSSLSTPSEPLSPTSSLGEERN ⁷³⁷	S710
Heat-schock protein beta-1	HSPB1	⁸⁰ QLSSGVSEIR ⁸⁹	S82
Phosphorylase B kinase regulatory α subunit	PHKA1	⁹⁷² SVRPTDSNVSPAISIHEIGAVGATK ⁹⁹⁶	S972
LIM domain-binding protein 3	LDB3	¹⁸⁹ DLAVDSASPVYQAVIK ²⁰⁴	Y199*
MYC box-dependent-interacting protein 1	BIN1	²⁹⁶ SPSPDGDSPAATPEIR ³¹¹	S298
Myoglobin	MB	⁶⁵ HGATVLTALGGILK ⁷⁸	T68*, T71*
Myomesin 1	MYOM1	⁶³ RASASSSQQASQHALSSEVSR ⁸⁴	S65*
Myosin binding protein C, slow type	MYBPC1	⁵⁷ KDSDWTLVETPPGEEQAK ⁷⁴	S59*
Myosin binding protein C, fast type	MYBPC2	³⁷ EAPPEDQSPTAEPTGVFLK ⁵⁶	S44*
Pyruvate dehydrogenase, E1 component α subunit	PDHA1	²⁸⁹ YHGHSMSPGVSYSR ³⁰²	Y289, T293
RAS GTPase-activating protein-binding protein 1	G3BP1	²³⁰ SSSPADIAQTVQEDLR ²⁴⁷	S232
Sarcoplasmic reticulum His-rich calcium-binding prot.	HRC	¹¹³ VGDEGVSGEEVFAEHGGQAR ¹³²	S119*
Sarcoplasmic reticulum His-rich calcium-binding prot.	HRC	¹⁵⁷ SHSHQDEDEDEVVSEHHHHILR ¹⁷⁹	S170*
Smoothelin-like 2	SMTNL2	³⁴² SQSFQVAVASASSIK ³⁵⁴	S344*

¹The sequence location of each peptide is indicated in superscript.

²Sites marked with “*” appear to be novel.

Figure 1

A

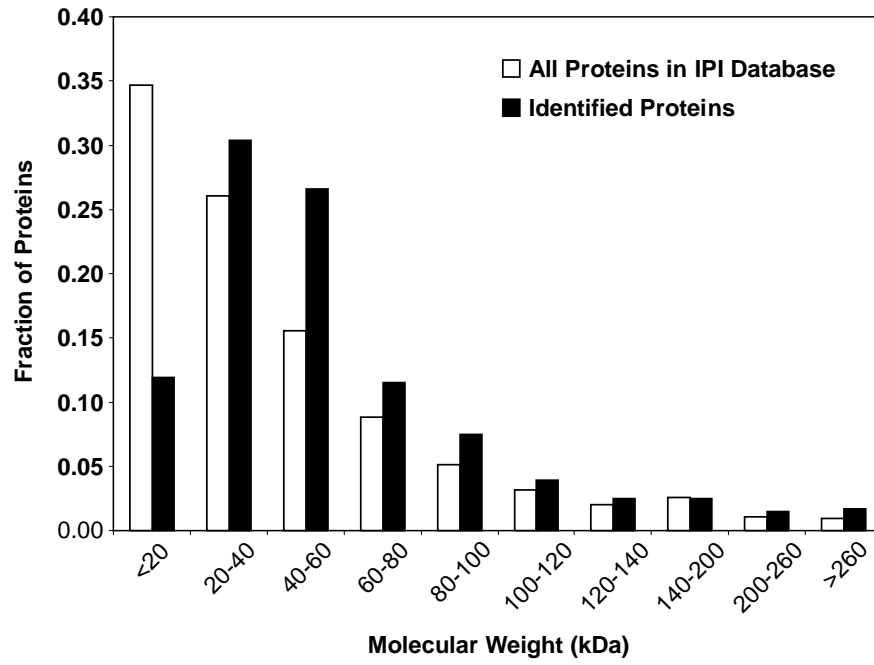


Figure 1

B

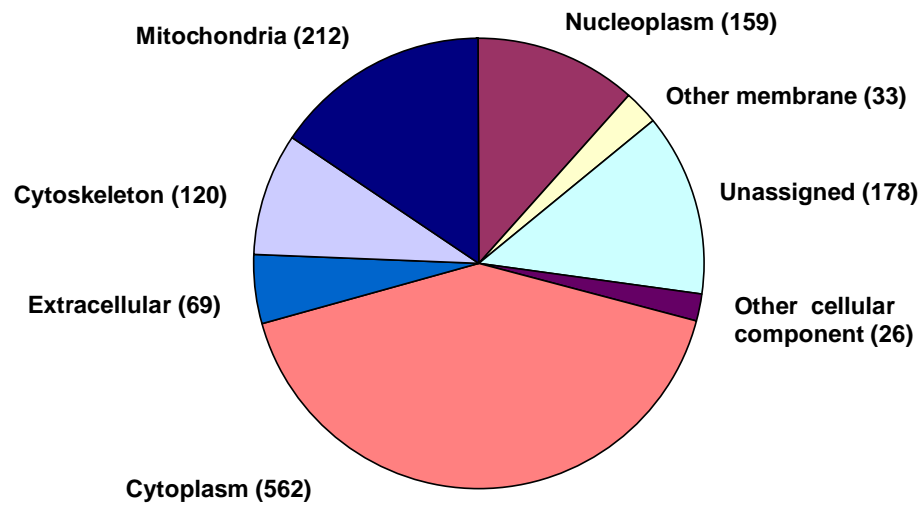
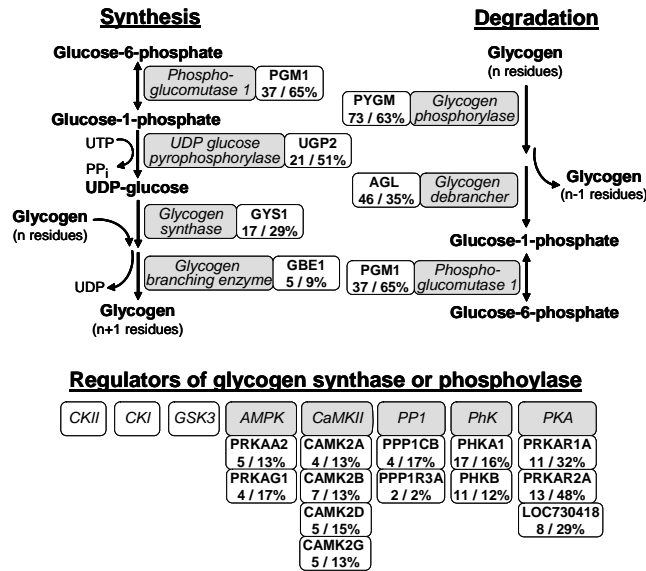
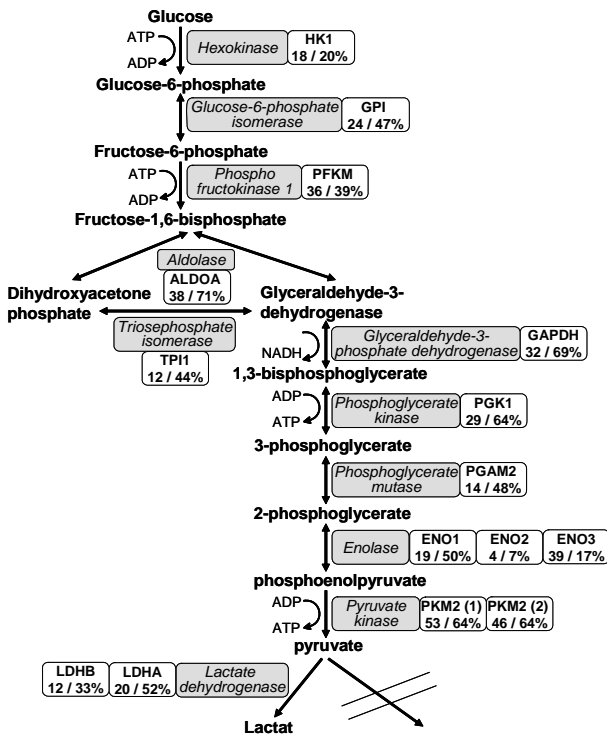


Figure 2

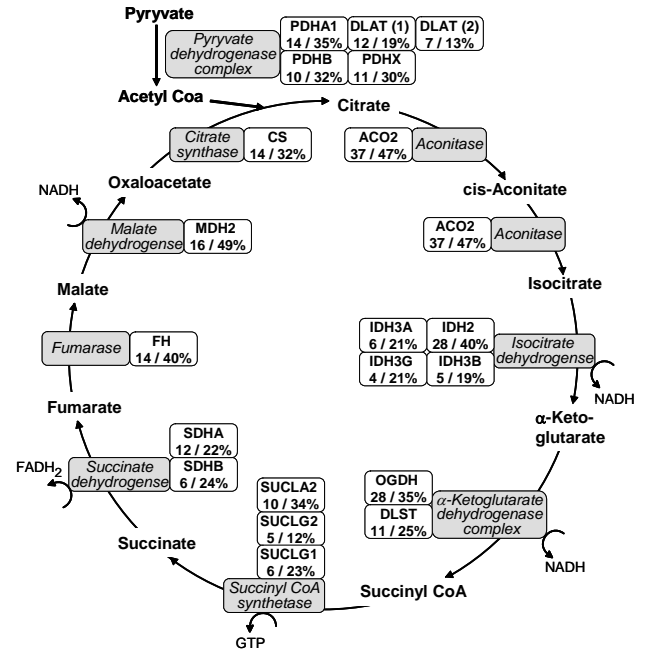
A Glycogen metabolism



B Glycolytic pathway



C Citric acid cycle



D Fatty acid transport and oxidation

